Nuclear Instruments and Methods 212 (1983) 13–21
North-Holland Publishing Company

TRANSVERSE BEAM CAVITY INTERACTION. Part I: Short range forces *

T. WEILAND

DESY, Notkestrasse 85, D2000 Hamburg 52, Germany

Received 26 November 1982

The transverse interaction between a bunch of charged particles and cylindrically symmetric accelerating structures is studied in three steps. The particle motion is influenced by short range forces and long range forces. The short range forces are calculated by solving Maxwell's equations in the time domain including the presence of free moving charges passing an arbitrarily shaped structure off axis. The long range forces are dominated by resonant modes in cavities. These forces are computed in frequency domain by evaluating eigenmodes and eigenfrequencies. Since only high energy particles are considered, the particle motion, which is affected by both forces, can be studied seperately using simple models and computer simulations.

This first paper deals with the computation of short range forces.

1. Introduction

The performance of high energy electron/positron storage rings and linear accelerators is strongly limited by current dependent phenomena. With increasing the number of particles per bunch the self excited electromagnetic fields increase and thus the beam environment interaction is enhanced. The most severe phenomena in storage rings is the transverse instability [1]. The transverse instability is likely to be dominated by the transverse impedance of the accelerating cavities. For simplicity we assume that all accelerating structures and other objects seen by the beam are cylindrically symmetric with an arbitrary shape in the r–z plane. The study of the transverse beam environment interaction can be split into three separated subjects since the particle density varies slowly in time:

i) *Short range forces.*
These forces are excited whenever a bunch traverses a structure off axis. They do not depend on the quality factor of a cavity but only on the shape of the structure.

ii) *Long range forces.*
After a bunch has passed a cavity resonant fields will remain with a certain frequency and decay rate. In a storage ring and a linear accelerator a following bunch (or the same bunch again) will interact with these fields.

iii) *Particle dynamics.*
All forces are causal and the particle distribution does not change fast compared to the build up time of the forces since only high energy particles are considered. Thus the dynamics can be studied separately using simple models and computer simulations.

In this paper a method for the computation of short range forces will be described which is based on the BCI method and program [2,3]. Since the structures are assumed to be cylindrically symmetric, all fields can be expressed in terms of dipole, quadrupole, etc. components with respect to the azimuthal coordinate. This fact enables a "quasi" three-dimensional computation and thus a fast computer code. For a small offset of the bunches from the symmetry axis the dipole forces are dominant. A consideration of the first two azimuthal momenta seems to be sufficient.

* Editor's note: This paper, which was originally published as a DESY report (DESY 82-015, March 1982) is reprinted here for the readers' convenience.

0167-5087/83/0000–0000/$03.00

2. Mathematical method

A bunch of charged particles with velocity βc in the z direction is described by the longitudinal line charge density $\lambda_s(s)$ having no transverse dimensions. If the bunch passes a cylindrically symmetric structure off axis at a distance a, the current density produced may be written as:

$$J(r, \varphi, z, t) = \frac{\beta c \lambda_s(z - \beta c t)}{2\pi a} \sum_{m=-\infty}^{+\infty} \cos m\varphi \, \delta(r - a) e_z. \tag{1}$$

Thus the electromagnetic fields excited by the bunch can also be written in terms of sinusoidal azimuthal dependence. Choosing the origin at the bunch as $\varphi = 0$ we have in general all six components of the electromagnetic field:

$$\begin{aligned} E_r(r, \varphi, z, t) &= E_r^{(m)}(r, z, t) \cos m\varphi, & H_r(r, \varphi, z, t) &= H_r^{(m)}(r, z, t) \sin m\varphi, \\ E_\varphi(r, \varphi, z, t) &= E_\varphi^{(m)}(r, z, t) \sin m\varphi, & H_\varphi(r, \varphi, z, t) &= H_\varphi^{(m)}(r, z, t) \cos m\varphi, \\ E_z(r, \varphi, z, t) &= E_z^{(m)}(r, z, t) \cos m\varphi, & H_z(r, \varphi, z, t) &= H_z^{(m)}(r, z, t) \sin m\varphi. \end{aligned} \tag{2}$$

From here on the upper index m will be omitted. The only geometry that can be treated half analytically is the infinite chain of "pill-box" cavities with beam tubes inbetween [4]. Since there is no way to solve for arbitrarily shaped structures without using a computer we will apply a mesh method to the problem. Basis for the method is the FIT-algorithm [5,6] which has been successfully applied to the case of an on axis beam [2,3].

The component of the fields are replaced by their values on a finite number of grid points using the locations described in ref. 7, see also fig. 1. The nodes are numbered first in z then in r direction linearly

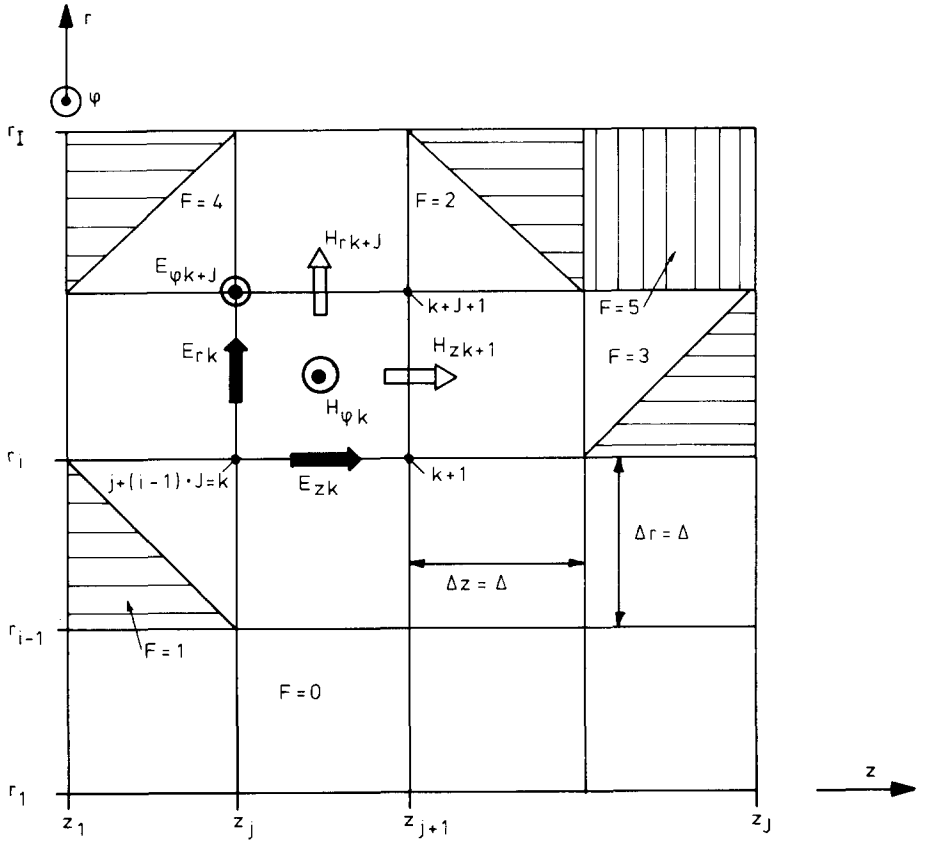

Fig. 1. The mesh used in the $r-z$ plane with equal steps in both directions. The mesh points are numbered linearly first in z and then in r direction. The filling index is F and may have values between 0 and 5 and thus F_k defines the boundary of the structure.

increasing. All the unknown values are put into vectors:

$$\boldsymbol{e} = \left(E_{r1}, \ldots, E_{rN}, E_{\varphi 1}, \ldots, E_{\varphi} N, E_{z1}, \ldots, E_{zN}\right)', \qquad \boldsymbol{h} = \left(H_{r1}, \ldots, H_{rN}, H_{\varphi 1}, \ldots, H_{\varphi N}, H_{z1}, \ldots, H_{zN}\right)'. \tag{3}$$

N is the total number of mesh points and the dimension of the two vectors is $3N$. Applying finite integrations to Maxwell's equations:

$$\iint\left(\epsilon_0 \dot{\boldsymbol{E}} + \boldsymbol{J}\right) \cdot \mathrm{d}\boldsymbol{A} = \oint \boldsymbol{H} \cdot \mathrm{d}\boldsymbol{s}, \qquad \iint\left(-\mu_0 \dot{\boldsymbol{H}}\right) \cdot \mathrm{d}\boldsymbol{A} = \oint \boldsymbol{E} \cdot \mathrm{d}\boldsymbol{s}, \tag{4}$$

yields a set of two equivalent matrix equations for $\boldsymbol{e}$ and $\boldsymbol{h}$:

$$D_e\left(\epsilon_0 \dot{\boldsymbol{e}} + \boldsymbol{j}\right) = R_e \boldsymbol{h}, \tag{5}$$

$$D_h\left(-\mu_0 \dot{\boldsymbol{h}}\right) = R_h \boldsymbol{e}. \tag{6}$$

The vector $\boldsymbol{j}$ contains the driving current produced by the beam. (The full derivation of the above equations is given in the appendix.)

The time axis is broken into pieces of Δt. The magnetic fields will be computed at times $t = n\Delta t$, the electric fields at half times $t = n\Delta t + \Delta t/2$. Due to this dual time axis the time derivatives in eqs. (5) and (6) can be replaced by:

$$\begin{aligned} \dot{\boldsymbol{e}}(n\Delta t) &= \left[\boldsymbol{e}(n\Delta t + \Delta t/2) - \boldsymbol{e}(n\Delta t - \Delta t/2)\right]/\Delta t, \\ \dot{\boldsymbol{h}}(n\Delta t + \Delta t/2) &= \left[\boldsymbol{h}(n\Delta t + \Delta t) - \boldsymbol{h}(n\Delta t)\right]/\Delta t. \end{aligned} \tag{7}$$

Thus both terms in the difference equations can be evaluated every half time step alternatively. Using the time argument of the vectors $\boldsymbol{e}$ and $\boldsymbol{h}$ as upper time index we can rearrange eqs. (5) and (6) to:

$$\boldsymbol{h}^{n+1} = \boldsymbol{h}^n - \frac{Y_0}{M\beta} A_h \boldsymbol{e}^{n+1/2}, \tag{8}$$

$$\boldsymbol{e}^{n+3/2} = \boldsymbol{e}^{n+1/2} + \frac{Z_0}{M\beta} A_e \boldsymbol{h}^{n+1} + \boldsymbol{j}^{n+1}, \tag{9}$$

with

$$Z_0 = \sqrt{\mu_0/\epsilon_0}, \qquad Z_0 Y_0 = 1,$$

M = number of time steps/mesh step, $M = \Delta z/(\beta c \Delta t)$, Δz = step size of the mesh. The sparse matrices A_h and A_e have elements of very simple structure and need not to be stored during a computation.

Starting with $\boldsymbol{e}^{0.5} = \boldsymbol{h}^0 = \boldsymbol{j}^0 = 0$. the recursive eqs. (8) and (9) enable a computation of the total electromagnetic field at all spatial locations and for all times by simple multiplications of matrices with vectors already known. The procedure is so far identical to the BCI-code with the only difference that twice as many field components are used.

3. The open boundary condition and stability

In order to enable the open boundary condition described in ref. 3 we need to know the electromagnetic field of a bunched beam in an infinitely long cylindrical beam pipe of radius R (fig. 2), with a as off-axis distance each component of the total field can be derived from the two potentials

$$\begin{aligned} \phi_1 &= -\sum_{m=-\infty}^{+\infty} \frac{\lambda_s(s) c\beta}{2\pi m}\left[\left(\frac{a}{R}\right)^{2m} - 1\right]\left(\frac{r}{a}\right)^m \sin m\varphi; \quad 0 \leqslant r \leqslant a, \\ \phi_2 &= -\sum_{m=-\infty}^{+\infty} \frac{\lambda_s(s) c\beta}{2\pi m}\left[\left(\frac{a}{R}\right)^m \left(\frac{r}{R}\right)^m + \left(\frac{a}{R}\right)^m\right] \sin m\varphi; \quad a \leqslant r \leqslant R, \\ &\text{with } \boldsymbol{H} = -\nabla\phi, \qquad \beta \approx 1. \end{aligned} \tag{10}$$

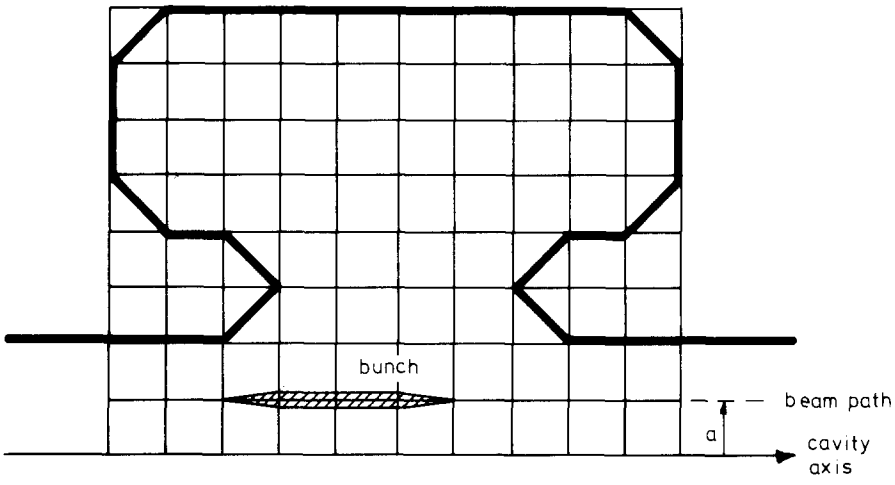

Fig. 2. An example of a cavity with infinitely long beam tubes on both sides. The bunch passes at a distance a away from the cavity axis.

The electric field is not needed. Thus an open boundary condition can be established in the same sense as in the case of longitudinal fields. Here in addition to the inhomogeneous H_φ components the radial fields are needed.

This boundary condition simulates infinitely long side tubes and does not need tapers of infinitely conducting metal to terminate the structure.

All considerations concerning the numerical stability of the time iteration apply in the same way as in the longitudinal case [2,3]. Since a "quasi" third dimension has been introduced an additional term has to be added. For equal step sizes in r and z stability requires the time steps to satisfy:

$$c\Delta t \leqslant \frac{\Delta z}{\sqrt{2+m}} \times \begin{cases} 1/\sinh(\pi/2) & \text{"open"}, \\ 1 & \text{"closed"}. \end{cases} \tag{11}$$

Since charge conservation requires an integer relation between time step size and space step size the condition may be rewritten in terms of M = time steps/mesh step [2]:

$$M \geqslant \frac{1}{\beta}\sqrt{2+m} \times \begin{cases} \sinh(\pi/2) & \text{"open"}, \\ 1 & \text{"closed"}. \end{cases} \tag{12}$$

The above equation implies that the number of cycles to be executed increases with increasing the angular momentum m. Since m is usually limited to 1 or 2, this does not increase the computation time significantly.

4. The computer code TBCI

Starting from the existing program for cylindrically symmetric fields (BCI) the transverse version has been established by introducing the new additional three field components. By some improvements the total length of the source was reduced significantly.

For transverse fields no graphical output is foreseen * in order to provide memory for the additional field components without increasing the total memory of the code. Thus the overall size of the program in the small version (20 000 grid nodes) could be kept constant at 800 kbyte on an IBM 370/168. The big version using 50 000 mesh points allocates less than 1500 kbyte.

* The version of TBCI distributed since May 1982 does have graphical output for the transverse fields as well without an increase in memory.

The cpu time consumption for transverse fields is increased by roughly a factor 2 compared to the longitudinal case. An average run on an IBM 370/168 with 20000 grid points needs 300–400 s including the computation of the wake forces.

All computed results such as fields and forces may be stored on external files for further manipulation by a set of utility programs.

The output of the code contains mainly the fields and the stored energy as a function of time as well as the transverse and the longitudinal wake potentials.

Self-checking routines have been implemented for independent control of the correctness of the code as well as for control of the proper solution of Maxwell's equations.

5. Examples

During the time when a bunch traverses a cavity electromagnetic fields act on the bunch as a function of time and each particle in the bunch will feel a different force. Since we assumed that the bunch shape does not vary during the passage only the total distribution of the forces after the passage is of interest. Theses time independent forces are then functions of the longitudinal position inside the bunch. They are normalized to the total charge in the bunch and usually called "wake potentials". The forces depend also on the shape of the bunch $\lambda(s)$ and on the radiation position r_1 at which the bunch traverses off axis the cavity. Independent of r_1 the forces may be integrated at a radial position r_2. For cavities with infinitely long side tubes (open boundary condition) it is found that the wake potentials scale exactly as they do in infinitely repeating structures [4]:

$$w_\perp(r_1, r_2, m, s) \propto w_\perp(m, s) r_1^m r_2^{m-1} \text{ (transverse)}$$
$$w_\parallel(r_1, r_2, m, s) \propto w_\perp(m, s) r_1^m r_2^m \text{ (longitudinal)},$$

with $r_1, r_2 \leqslant$ beam tube radius. Thus the normalized wake potentials have the dimensions

$$\left[w_\perp(m, s)\right] = \mathrm{V/As/m}^{2m-1}, \qquad \left[w_\parallel(m, s)\right] = \mathrm{V/As/}m^{2m}.$$

For the PETRA accelerating cavity [8], the future PETRA cavity [9] and the LEP accelerating cavity [10] the dipole wake potentials are shown in figs. 3, 4 and 5 for Gaussian bunches with r.m.s. length $\sigma = 3$ cm. All three wake potentials look very similar. The transverse force is roughly proportional to the particle density but shifted to "later" particles.

The dipole and quadrupole wake forces are shown in fig. 6 for a single cell of the PETRA cavity and a Gaussian bunch with $\sigma = 2$ cm. It can be seen that for small offsets the dipole force is dominant. The peak values relate as:

$$\hat{w}_\perp(m = 2)/\hat{w}_\perp(m = 1) \sim 250(r_1/m)(r_2/m).$$

The linear betatron tune shift due to the wake potentials of the cavities can be obtained from:

$$\Delta Q = -\frac{1}{4\pi}\frac{1}{E_0/e}\langle\beta\rangle_{\mathrm{rf}}\int_{-\infty}^{+\infty} w_\perp(s)\lambda(s)\,\mathrm{d}s,$$

with
$w_\perp(s)$ total wake potential of all cavities in the ring,
$\langle\beta\rangle_{\mathrm{rf}}$ average value of the beta function in the cavities,
E_0 particle energy,
$\lambda(s)$ line charge density of the bunch.

For a Gaussian bunch with r.m.s. length $\sigma = 2$ cm the tune shift due to 60 PETRA cavities at injection energy (7 GeV) becomes ($\langle\beta\rangle = 15$ m):

$$-\Delta Q \approx 0.0017/\mathrm{mA} \triangleq 215\ \mathrm{Hz/mA}.$$

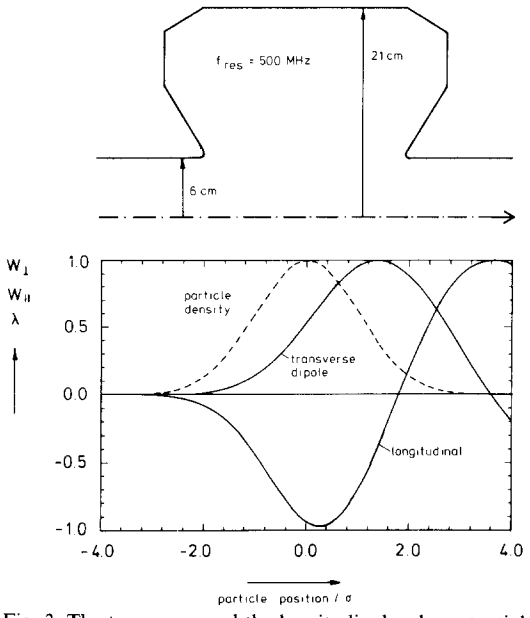

Fig. 3. The transverse and the longitudinal wake potentials due to a single cell of the PETRA cavity as a function of particle position.
Scale transverse = 8.2×10^{12} V/As/m.
Scale longitudinal = 9.8×10^{13} V/As/m^2.

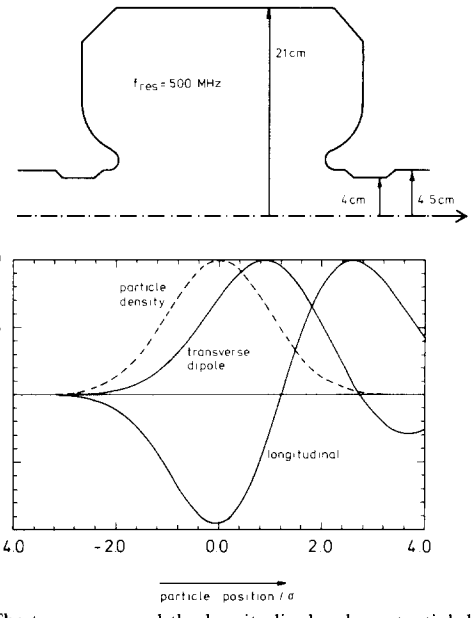

Fig. 4. The transverse and the longitudinal wake potential due to a single cell of the future PETRA cavity.
Scale transverse = 1.2×10^{13} V/AS/m.
Scale longitudinal = 1.8×10^{14} V/As/m^2.

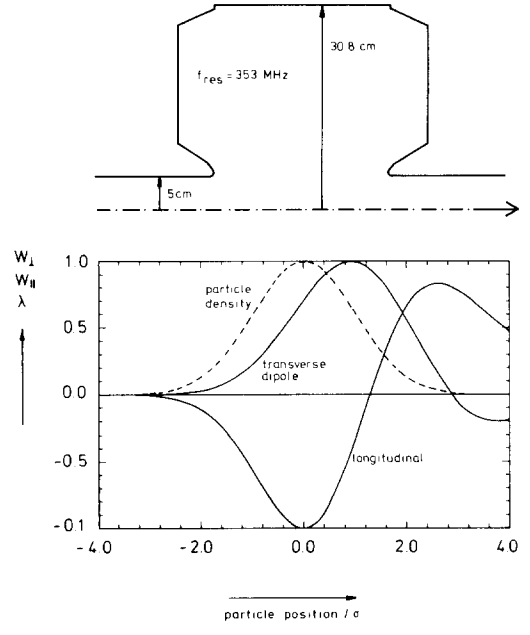

Fig. 5. The transverse and the longitudinal wake potential due to a single cell of the LEP cavity.
Scale transverse = 1.1×10^{13} V/As/m.
Scale longitudinal = 1.4×10^{14} V/As/m^2.

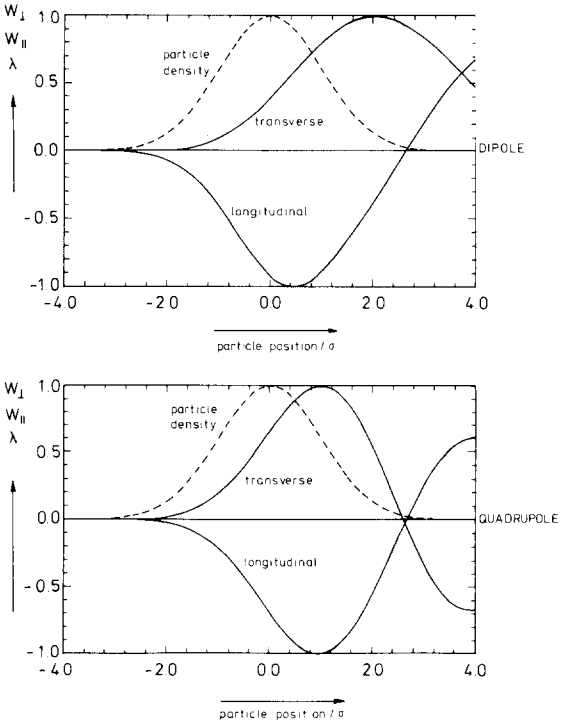

Fig. 6. The dipole and quadrupole wake potentials due to a single cell of the PETRA cavity.
Scale dipole trans. = 1.0×10^{13} V/As/m; long. = 1.3×10^{14} V/As/m^2.
Scale quad. trans. = 2.6×10^{15} V/As/m^3; long. = 2.2×10^{16} V/As/m^4.

From measurements the total tune shift is known to be [11]:

$$-\Delta Q \approx 0.0034/\mathrm{mA} \hat{=} 450\ \mathrm{Hz/mA}.$$

One can conclude from these numbers that the total tune shift due to the vacuum system in PETRA is roughly equal to the effect of 60 cavities. A detailed investigation of the tune shifts as a function of bunch length will follow in a later paper. In general it is found that the dipole tune shift decreases for very short bunches but the amplitude of the wake force increases.

For LEP Phase II [10] and a bunch length $\sigma = 3$ cm the betatron tune shift at injection energy reaches the value:

$$\Delta Q = -0.5/\mathrm{mA},$$

for

$$E_0 = 20\ \mathrm{GeV},\ n_{\mathrm{cav}} = 768\ (5\text{-cell cavities}),$$

$$\langle\beta\rangle_{\mathrm{rf}} = 50\ m, \qquad T_0 = 88.9 \times 10^{-6}\ \mathrm{s\ (rev.\ time)}.$$

6. Conclusions

The method described enables by means of the computer code TBCI a computation of deflecting forces acting on a bunch of charged particles passing off axis a structure of cylindrical symmetry. The shape of the structure may be arbitrary in the r–z plane and may have infinitely long beam tubes on both sides. Since the self-induced transverse forces are likely to limit the performance of future storage rings and linear accelerators the quantitative prediction of such forces is necessary for a design of such a machine.

Appendix

A.1. Difference equations in the vacuum

Solving the integrals in Maxwell's equations with a first order approximation yields linear equations for the electric and magnetic field components. We will assume first that the mesh point with number k lies entirely in vacuum and no boundary is near to it. Integrating the first eq. (4) on the left hand side over the area in the φ–z plane defined by (see fig. 7): $A = 0, \psi) \times (z_j - \Delta/2, z_i + \Delta/2)$ at $r = (i - 1/2)\Delta$ yields:

$$\iint \epsilon_0 \boldsymbol{E} \cdot \mathrm{d}\boldsymbol{A} \cong \epsilon_0 E_{rk} (i - 1/2)\Delta^2 \int_0^{\psi} \cos m\varphi\ \mathrm{d}\varphi. \tag{13}$$

Integrating the right hand side of these equations along the boundary of the area A yields:

$$\int \boldsymbol{H} \cdot \mathrm{d}\boldsymbol{s} \cong (i - 1/2)\Delta \int_0^{\psi} \cos m\varphi\ \mathrm{d}\varphi \left(H_{\varphi k-1} - H_{\varphi k} \right) + \Delta \sin m\varphi H_{zk}. \tag{14}$$

Replacing the time derivative according to eq. (7) in eq. (13) and equating both results finally yields an equation which enables the computation of E_{rk} from the earlier value and from three magnetic components in the neighbourhood:

$$E_{rk}^{n+3/2} = E_{rk}^{n+1/2} + \frac{Z_0}{m\beta} \left(\frac{2m}{2i-1} H_{zk} + H_{\varphi k-1} - H_{\varphi k} \right). \tag{15}$$

In a similar way the two other equations may be found for the azimuthal and the longitudinal component of the electric field.

Solving the second Maxwell equation on areas perpendicular to magnetic field components yields the

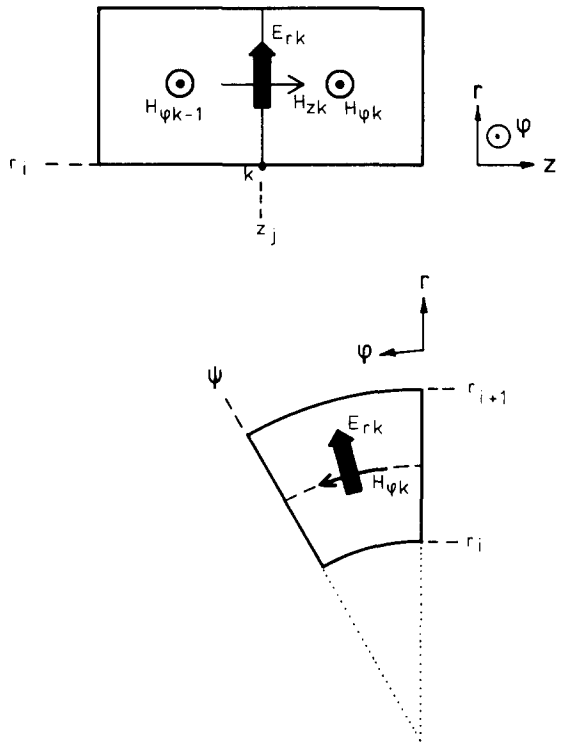

Fig. 7. The area of integration for the first Maxwell equation yielding an equation for the radial electric field component as a function of the azimuthal and longitudinal magnetic fields in the direct neighbourhood of mesh point number k.

second set of three equations for the evaluation of the magnetic fields. The full set which is necessary for the calculation of all the fields at a time step $n+1$ and $n+3/2$ reads:

$$H_{rk}^{n+1} = H_{rk}^{n} - \frac{Y_0}{M\beta}\left(E_{\varphi k}^{n+1/2} - E_{\varphi k}^{n+1/2} - \frac{m}{i-1} E_{zk}^{n-1/2} \right). \tag{16}$$

$$H_{\varphi k}^{n+1} = H_{\varphi k}^{n} - \frac{Y_0}{m\beta}\left(E_{zk}^{n+1/2} - E_{zk+j}^{n+1/2} + E_{rk+1}^{n+1/2} - E_{rk}^{n+1/2} \right), \tag{17}$$

$$H_{zk}^{n+1} = H_{zk}^{n} - \frac{Y_0}{M\beta}\frac{2}{2i-1}\left[iE_{\varphi k+J}^{n+1/2} - (i-1)E_{\varphi k}^{n+1/2} + mE_{rk}^{n+1+2} \right] \tag{18}$$

$$E_{rk}^{n+3/2} = E_{rk}^{n+1/2} + \frac{Z_0}{M\beta}\left(H_{\varphi k-1}^{n+1} - H_{\varphi k}^{n+1} + \frac{2m}{2i-1} H_{zk}^{n+1} \right), \tag{19}$$

$$E_{\varphi k}^{n+3/2} = E_{\varphi k}^{n+1/2} + \frac{Z_0}{m\beta}\left(H_{rk}^{n+1} - H_{rk-1}^{n+1} + H_{zk-J}^{n+1} - H_{zk}^{n+1} \right), \tag{20}$$

$$E_{zk}^{n+3/2} = E_{zk}^{n+1/2} + \frac{Z_0}{M\beta}\left(\frac{2i-1}{2i-2} H_{\varphi k-J}^{n+1} - \frac{2m}{2i-2} H_{rk}^{n+1} \right). \tag{21}$$

The source term comes into eq. (21) and has to be added at the radial position of bunch:

$$E_{zk}^{n+3/2} = E_{zk}^{n+1/2} - \lambda_k^{n+1} \frac{1}{i-1} \frac{1}{m\pi\Delta z \epsilon_0} \frac{1}{1+\delta_{0m}}, \tag{22}$$

$\delta_{0m} = 1$ for $m = 0$; $= 0$ for $m \neq 0$.

The above equations guarantee that the electric and the magnetic field stay source free with increasing

time. This may easily be checked by integrating the electric field over the surface of the volume:

$$V_e = (r_i - \Delta/2;\ r_i + \Delta/2) \times (0;\ \psi) \times (z_j - \Delta/2;\ z_j + \Delta/2),$$

and replacing the electric components by magnetic ones according to eqs. (19)–(21). This yields identical zero. Since the computation is never infinitely accurate there will be a small charge resulting from rounding off errors. In order to check the proper coding of the field equations this charge on any mesh point may be divided by the total charge in the bunch. The so computed relative parasitic charge is small compared to unity.

Integrating the magnetic field over the surface of a mesh cell:

$$V_h = (r_i;\ r_i + \Delta) \times (0;\ \psi) \times (z_j;\ z_j + \Delta)$$

gives the total magnetic charge in this cell. Setting the magnetic force equal to the electric force gives an equivalent magnetic charge to the total charge in bunch Q_e:

$$Q_m = Z_0 Q_e.$$

Relating the parasitic magnetic charges in the mesh cells to the above equivalent charge yields the second number which is small compared to unity.

Both parasitic effects are used in the computer code TBCI in self-checking routines which check proper coding and computation independently.

A.2. Boundary conditions

The boundary condition is defined by the material index F in each cell, see fig. 1. The electric field components are located in such a way that they either are parallel to a boundary surface or that they do not touch such a surface at all. This enables an easy implementation of the boundary condition. When a electric field component lies parallel to a boundary surface it will not be evaluated and thus stays zero for all times.

The magnetic field components in radial and longitudinal direction are either perpendicular to a metallic surface or do not touch a boundary at all. Thus we proceed in the same way as before and do not calculate those components which are zero by boundary condition. The only component which has to be looked at in more detail is the azimuthal magnetic field component. If the mesh cell if entirely filled ($F = 5$) with infinitely conducting metal the field is identical zero and will not be calculated. If the cell is entirely filled with vacuum eq. (17) is used. There is no need to care about the boundary conditions for the electric field components involved here. If the cell is filled with a triangular metal the area of integration is halfed and thus all coefficients on the right hand side of eq. (17) have to be doubled. Again there is no need to ask whether the electric fields involved are anyway zero or not.

Summarizing the above comments we find that boundary conditions do not cause any complication. In order to achieve a even faster execution one may omit the boundary conditions for the magnetic fields. In the time domain it is sufficient to fulfill the boundary conditions for only one of the fields E or H.

References

[1] R.D. Kohaupt, DESY H1/74-02 (May 1984) and DESY 80/22 (March 1980).
[2] T. Weiland, 11th Int. Conf. on High energy accelerators, Geneva (1980) p. 570.
[3] T. Weiland, CERN/ISR-TH/80-46 (1980) and CERN/ISR-TH/80-45 (1980).
[4] K. Bane and P.B. Wilson, 11th Int. Conf. on High energy accelerators, Geneva (1980) p. 592.
[5] T. Weiland, Arch. Elektr. Übertrag.-tech. 31 (1977) 116.
[6] T. Weiland, Kleinheubacher Berichte 24 (1981) 37.
[7] T. Weiland, Darmstädter Diss. D17, Technische Hochschule (1977).
[8] H. Gerke, et al., DESY PET-77-08.
[9] H. Gerke, private communication.
[10] The Lep Study Group, CERN/ISR-LEP/79-33.
[11] R.D. Kohaupt and T. Weiland, DESY M82-07.